Development and Deployment of a Wireless Network Testbed, and Evaluation of Wireless Systems for Airport Applications

Final Technical Report for the FAA Spectrum Office

FAA Technical Center Grant # 06-G-005

August 2007

David W. Matolak, Ph.D.
Associate Professor

School of EECS/Avionics Engineering Center

Ohio University

Athens, OH 45701

phone: 740.593.1241

fax: 740.593.0007

email: matolak@ohiou.edu

Summary

This document describes completed work on the investigation of the employment of new wireless network technologies for aviation applications on airport surface areas (ASAs). The wireless technologies studied are those in the new wireless metropolitan area network (WMAN) family developed by the IEEE standards organization, denoted the IEEE 802.16 standard(s). The particular version of this standard is 802.16-2004, which was recently enhanced to 802.16e, primarily to enable support of mobility. The primary goal of this project was to evaluate this networking technology, deployed in the 5 GHz microwave landing system extension (E-MLS) band in ASAs. This evaluation was to be both analytical and experimental.

Due to *un*availability of actual networking equipment during the entire project period, no experimental work was completed. Thus, this project focused instead on analysis and computer simulation results for this technology in the desired application. These results hence constitute the primary contributions of this report, and of the interim report of December 2006.

After a short review of the original project objectives, we provide a short description of the project status, with regard to the goal of deploying and testing an experimental network (testbed). A brief review of the standard, and configurations suitable for the airport surface area environment, is then provided. We also provide a very short discussion of some recent pertinent literature on 802.16 that is of interest in future ASA deployments. This is followed by some new example analytical and computer simulation results. As in the interim project report, our results use the statistical wireless channel models we recently developed for this environment, and thus these results represent the most accurate set of physical and medium access control layer performance results yet presented for 802.16 deployed in the ASA environment. We conclude the report with a summary, and some recommendations for future continuation of the project.

1. Summary of Original Project Objectives

As listed in the original project proposal [1], the original project objectives were to configure, develop, and deploy a wireless network testbed to study its use for airport surface area applications. The two types of efforts planned were a "proof of concept" part, and an experimental part. These are briefly described in the interim project report [2]. Appendix B of [2] contains a description of the proof of concept portion, which was essentially to show feasibility of 802.16 modems to transfer data of various types, reliably, on the airport surface. For completeness, we re-state these original "proof of concept" objectives here. They were to demonstrate

1. use of the 5 GHz frequency band to transport information on the airport surface;
2. transmission/reception of high-rate data in this band with low error probability;
3. attainment of the previous two items with both fixed and mobile platforms;
4. attainment of the previous three items with technologies based upon commercial wireless standards.

Although these objectives were not strictly achieved because we had no networking hardware, we have, through our analyses and simulations, shown that in principle all of these objectives are feasible to attain.

The experimental portion of the project was to extend the "proof of concept" objectives to move closer to the goal of actually using 802.16 in the ASA environment. The original experimental objectives are repeated here:

1. validate models and specifications for the system components;
2. explore system configuration/setup options to enable the network to meet some basic, and possibly "advanced" requirements;
3. enable exploration of advanced radio and signal processing techniques to improve performance, reliability, capacity, and security of the network.

As with the proof of concept" objectives, these experimental objectives also could not be met without networking equipment. Yet again, the analytical and simulation results we have obtained represent a good initial step toward fulfilling them. We have in principle achieved the "basic" requirements part of the second objective. Also, our continued study of the (lengthy and detailed) 802.16 standard has provided us with much knowledge required for pursuing the 3rd experimental objective. This objective can be re-stated as devising various physical layer (PHY) and medium access control (MAC) layer augmentations in order to best configure the 802.16 system for the ASA environment and envisioned applications. (These augmentations include adaptive bandwidth, adaptive center frequency, and adaptive data distribution across subcarriers to optimize the system performance, in addition to assessing the system performance in the presence of interference, unintentional or otherwise.)

Appendix A of [2] contains the original project schedule, which could not be followed because of the absence of network equipment. In short, the project milestones were to consist of acquisition of a small set of networking equipment, e.g., one base station and several subscriber stations, followed by laboratory testing. Laboratory work was to be followed by a set of basic functionality tests at a small airport (Ohio University's airport), and finally deployment and testing at a large airport (e.g., Cleveland Hopkins). Given that no equipment was available, we were able to extend the project's funding an additional three months. During this time, analysis and computer simulations were conducted.

2. Work Status

As in the interim report, we divide this section into two parts: the first part describes the status of acquiring the networking equipment, and the second part describes our completed work on analysis and simulations. Some additional detail on the history of the search for networking equipment is provided in [2].

2.1 Status: Acquisition of Networking Equipment

There are numerous potential vendors for 802.16 equipment. A look at the "WiMax Forum" website [3] indicates that dozens—perhaps hundreds—of vendors will be selling this equipment. (We note that WiMax is strictly an industry designation for the developed 802.16 hardware/firmware/software products, and that current plans are for these products to implement only a subset of the large number of possible 802.16 configurations.) Throughout the project, we contacted a large number of these vendors, both by phone and by email. A partial list of those vendors and "system integrators," chosen for their reputation and because of reasonably good advertising on their web sites, includes the following: Airspan, Alliance, Alvarion, Axxcelera,

Aperto, Fujitsu, Intel, Navini, Proxim, Redline, Siemens, and Wireless Connections. At one point we also discussed our desired system with representatives of the Wireless Internet Network Operators Group (WINOG), and also discussed the system we desired with representatives of several other companies at a large international communications conference [4]. (This included representatives of Intel, Inc., the leading manufacturer of the chip sets used in the 802.16 baseband and radio frequency (RF) subsystems.)

We found that, although some vendors currently have available 802.16e equipment that is either fully or partially compliant with the existing standard [5], all equipment operates at a different radio frequency (RF), either in the 2.4 or 3.5 GHz band. Operation in the 3.5 GHz band requires a license, but all vendors we contacted indicated that would not be a problem, at least for temporary use. Operation at 2.4 GHz would expose the system to interference from the widely used WLAN transmitters in this band (802.11b and 802.11g). Some vendors indicated that they may plan to make equipment that operates in a WLAN band just above the E-MLS band in the future (e.g., 5.15-5.2x GHz), but the actuality and timing of this depends on the highly volatile WLAN market, and on the schedules of chip set and firmware manufacturers. These schedules are, of course, not possible to accurately predict. At present, it appears unlikely that any 5 GHz 802.16 equipment will be available in 2007.

As we noted in [2], no vendors to whom we spoke were able to give us a concrete estimate of the time and funding it would take to shift the RF into the E-MLS band: several vendors provided us with rough estimates, ranging from a low value of $50,000 and 6-9 months to $500,000-$1 million and 12 months. Roughly six months into the project, we had considered using an older version of WLAN equipment—the widely used 802.11a standard, but given the requirements of the ASA environment, and the strong recommendation for use of 802.16 given in [6], we did not pursue this course. The interim report [2] provides an overview of the relative advantages and disadvantages of using either 802.11a or 802.16 equipment for the ASA applications. One of the disadvantages to both was *not* making explicit use of the E-MLS band, which is desired to show the aviation community's intent to exploit this band, and circumvent any attempts to re-allocate the band to other uses. Based upon the 2006 World Radio Conference, it appears that the E-MLS band has been protected for aviation use for the present.

As of the time of writing of this report, all vendors whom we contacted were unable to give us any assurance that even 3.5 GHz WiMax equipment would be available before October 2007. Various reasons for this were given, most often that the manufacturer of a subsystem (often one of the chip sets) was behind schedule.

2.2 Status: Network Analysis and Computer Simulations

We have worked throughout the project to familiarize ourselves with the 802.16 and 802.16e standards. As is well known, the standards specify the PHY and data link layer (DLL, specifically, the medium access control, MAC, convergence sublayer, and security sublayer) portions of the technologies, at the transmission end. This means that no specifications within the standards address receiver performance or reception techniques, which are left to equipment manufacturers (this is common for other technologies, e.g., cellular radio, as well). These voluminous standards afford the system engineer more options than are likely ever to be used in practice. In fact, even text books on the topic restrict their coverage somewhat [7].

One of our main goals in studying the standard, and in analyzing and conducting computer simulations of the PHY and MAC parts of the standard, was to gain a basic understanding of the technology. This includes the basic OFDM(A) modulation and its various options, the various forward error control (FEC) coding options, and the MAC layer scheduling and "interleaving" options. The second, project-directed goal, was to determine how the 802.16 system could be best configured for airport surface operation. We determined several OFDMA parameter sets useful for study as deployment configurations for the ASA environment. We selected these parameter sets based upon our measured channel characteristics and channel models [8], and upon the total available bandwidth in the E-MLS band. As has been noted elsewhere, e.g., [9], we began with the assumption that the approximately 60 MHz of E-MLS band spectrum will be allocated to multiple services. This includes point-to-point non-mobile data transfer (e.g., from airport sensors) and point-to-multipoint data transfer between mobile platforms. The simplest means to realize this division of band usage is via frequency division of the band into several channels. Because of this, we selected channel bandwidths on the order of 10 MHz and smaller.

As noted in [2], we have limited our study to a single "cell" with a point-to-multipoint (PMP) topology, in which multiple subscriber stations (aircraft, ground vehicles, etc.) connect with a single base station (mostly assumed to be the air traffic control tower, ATCT). Although the 802.16 standard provides for a mesh topology, this mode of operation greatly increases the number of conditions to investigate, and at this early stage, it is not clear if a mesh mode of operation is needed for the ASA applications. Based upon the standard, we analytically determined several of the most important bounds on system PHY parameters that would enable the system to accommodate the channel's delay spreads T_M (rms value σ_τ) and Doppler spreads f_D. As with cellular radio and other standards, the 802.16 standard specifies a small number of "basic" PHY parameters, from which dependent "derived" parameters are computed. The specification of both basic and derived parameters essentially defines the PHY configuration. Some of the basic parameters include the channel bandwidth, the size of the Fast Fourier Transform (FFT), the number of "used" subcarriers for different FFT sizes, and the ratio of guard time to symbol time. Some derived parameters include the sampling frequency, the "useful" symbol time, and the inter-subcarrier frequency spacing.

All these parameters, along with pilot symbol and subchannel mapping schemes, have been used to develop several sets of computer simulations. The 802.16 standard allows for a number of different pilot and subchannel mapping modes for flexibility in trading performance versus throughput (data rate and number of active users). The simulations enable us to conduct PHY performance analyses for several channel conditions, modulations, and numbers of active users. We have also investigated the use of several MAC layer scheduling schemes to assess quality of service (QoS) at this layer, primarily in terms of achievable data rate and error probability. Our simulations also include channel estimation at the receiver, for which we have developed and explored three algorithms. In the MAC layer results, we allow for two general "service classes, denoted "best effort" (BE) and "guaranteed performance" (GP).

Initially (i.e., in [2]) we focused upon worst case channel conditions, which corresponds to the non-line-of-sight (NLOS), large airport models of [8]. Those results illustrated some of the performance limits of the selected schemes in the ASA environment. In this report we extend the scope to include results for both medium, and small airports, still using the NLOS channel models. We also include new results on turbo FEC coding, and performance in the presence of in-band interference.

We also continue use of the following assumptions: (i) the band in which the single-cell network operates is free of adjacent channel WLAN interference and co-channel outside-system interference; (ii) nonlinear distortions (e.g., due to saturated RF power amplifiers) are negligible; and (iii) receiver carrier frequency and phase estimation is nearly perfect. For the PHY results, the simulation outputs are bit error ratio (BER) performance versus bit energy to noise density ratio (E_b/N_0). The MAC results show the number of supportable user signals in each of the two service classes, given specified BER and data rate requirements.

As is often the case with computer simulations, it is easy to state that they are "incomplete," and more conditions and options can almost always be investigated. At this point we have a set of fairly general and easily modified computer programs, from which we have generated a representative set of example simulation results. These results provide examples of performance that can be expected in the ASA environment. *Many* more simulation results could easily be generated, but our intent here was not to produce dozens of simulation result plots solely for the sake of report length, but rather to provide illustrations of performance. For any future work, particularly if combined with experimental testing, additional simulations, tailored more precisely to the *specific* conditions of interest, can and ought to be done.

3. Network Technology Overview

In this section we provide a summary of the 802.16 standard, first in general terms, then with some specifics for ASA environment application.

3.1 General 802.16 Description

A brief description of the 802.16 standard was provided in [2]; herein for completeness we re-state some of that description, and provide additional detail. For a comprehensive description of the standard, we recommend the standard itself [3], or the new text [7]. Our focus in this report is on the physical layer, with some discussion on the data link layer. As with the 802.11a WLAN standard, the 802.16 standards employ orthogonal frequency division multiplexing (OFDM) [10], which is a multiple-carrier, block-based transmission scheme. The "e" version of the standard provides enhancements specifically aimed at supporting mobility via rapid power control, handoffs between cells, and adaptive transmission formats (both modulation type and FEC). These standards also specify a single-carrier option, but this is likely to be used only infrequently, for example when a system designer has exclusive access to a band and desires only point-to-point data transfer (using highly directional antennas). The multiple modulation schemes available in 802.16 are QPSK, 16-QAM and 64 QAM. The multiple FEC coding schemes are often "matched" to modulations, and as such have variable block sizes, various rates, and specific interleaving algorithms; these interleaving methods use both time and frequency domains.

Since in deployments on the airport surface area it is most likely that multiple platforms or user terminals (subscriber stations, designated SS in the standard) will be accessing the system dynamically, we have focused upon the multiple-access portion of the standard denoted OFDMA, with the MA designating multiple access. This part of the standard is configured to allow multiple SSs to communicate with a central base station (BS) (or bases), on a dynamic,

time- and frequency-shared basis, with different levels of quality of service (QoS). Thus any system user may at any time employ only a portion of the band, consisting of some fraction of the total number of carriers (subcarriers). As concluded in [6], the OFDMA scheme is well suited for use in the ASA environment, since multiple users will desire rapid access and reliable data transfer for arbitrary durations and a range of data rates, and with various levels of QoS. The standard allows for scalable channel bandwidth, the option of different FFT sizes, selectable slot and guard times to circumvent multipath dispersion, and several pilot symbol patterns for channel estimation. The FFT size specifies the number of subcarriers, and takes values from the set {128, 512, 1024, 2048}. The standard also describes several advanced transmission techniques, including multiple-input/multiple-output (MIMO) processing via antenna arrays, and turbo FEC. Throughout this work, we do not address MIMO techniques, but have included some results here on turbo FEC performance.

The OFDMA transmission system provides flexibility in subcarrier allocation, that is, in how the multiple users' data symbols and known control symbols are distributed in frequency. In the 802.16e standard, two mandatory distributed permutations for the OFDMA based air interface, partial usage of subchannels (PUSC), and full usage of subchannels (FUSC), are specified for subchannel allocation. (Generally speaking, a subchannel is a group of subcarriers in the frequency domain that spans a number of symbols in the time domain.) The distributed permutation scheme reduces the probability of experiencing bad channel fading on all subcarriers of each subchannel allocated to a given user. The permutation functions like an interleaver with a large block size, thus enabling the FEC to effectively achieve more coding gain than can be attained using contiguous subcarriers in each subchannel. The random permutation in subcarrier allocation also provides "statistically identical" channel qualities, thus fairness can be achieved among all active users. The standard also defines an optional adaptive modulation and coding (AMC) permutation, which uses contiguous zones in the time and frequency domains for a given user, providing vendors flexibility in choosing advanced scheduling algorithms.

A typical system structure is illustrated in Figures 1 and 2, for the uplink (SS to BS) direction of transmission. (Processing for the other direction of transmission is similar.) The input data is passed through the convolutional encoder, block interleaver, and the quadrature amplitude modulator (QAM) in sequence. The serial QAM symbols are then converted to parallel data streams on assigned data subcarriers and extra known pilot symbols are added onto the corresponding pilot subcarriers for estimation and detection purposes.

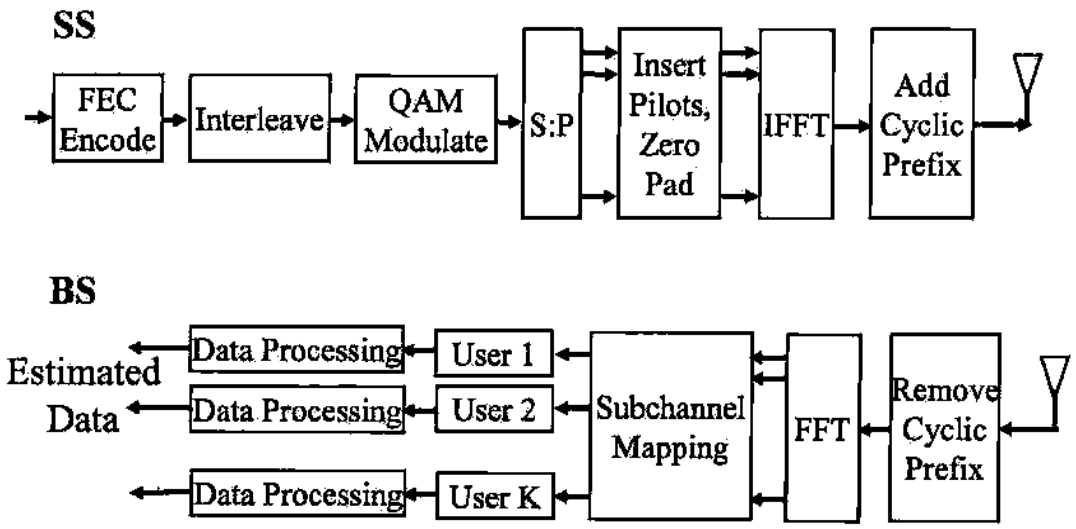

Figure 1. 802.16 uplink (SS to BS) PHY processing.

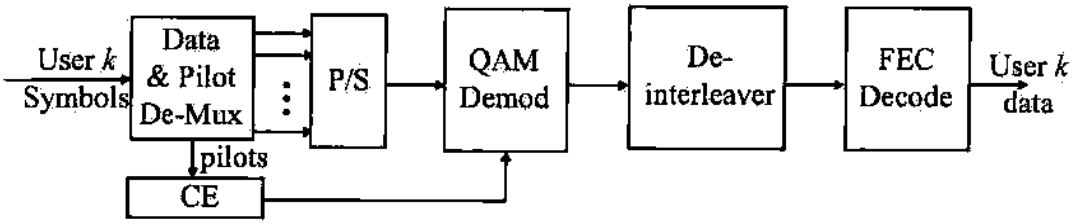

Figure 2. Final stages of k^{th} user uplink (SS to BS) PHY processing at BS (see Fig. 1).

For purposes of description, here we assume the number of subcarriers N=512 (we showed in [2] that this is a good choice—more will be said about this subsequently). After inverse fast Fourier transform (IFFT) at the transmitter, the resultant signal of the kth user can be written as

$$x_{kn}(i) = \sum_{m=-256}^{255} X_{kn}(m) e^{j2\pi im/N}, i = 0,1,\ldots,N-1 \tag{1}$$

where $x_{kn}(i)$ is the transmitted signal of the kth user on the ith time sample of the nth OFDMA symbol, and $X_{kn}(m)$ is the transmitted data symbol of the kth user on the mth subcarrier at the nth OFDMA symbol index. The data symbols $X_{kn}(m)$ appear from the QAM modulator output to the IFFT input in Figure 1. These data symbols can be expressed by

$$X_{kn}(m) = \begin{cases} d_{kn}(m), m \in I_{dk} \\ p_{kn}(m), m \in I_{pk} \end{cases} \tag{2}$$

where I_{dk} and I_{pk} are the index sets of data subcarriers and pilot subcarriers for the kth user, respectively. Note that subcarriers are not allowed to be shared among users in the frequency domain. Also, an "OFDMA symbol" is defined as the set of all simultaneously-transmitted data symbols on all active subcarriers, that is, the parallel collection of the $N_{used}+N_{pilot}$ data symbols X_{kn} sent during T_s (more will be said about these parameters in the next section). After IFFT, a cyclic prefix longer than the maximum delay spread of the channel is then inserted in $x_{kn}(i)$ to avoid the interference caused by multipath dispersion. These complex time domain samples are then upconverted to the carrier frequency, and amplified and sent to the antenna.

Here we assume all active users in the system are perfectly synchronized with the BS—procedures for ranging and synchronization are described in the standard. With $\tau=l/f_{sam}$ in the channel model from [8], with f_{sam} the sampling frequency, the received signal at the ith sample for the nth OFDMA symbol is

$$y_n(i)=\sum_{k=1}^{K}\sum_{l=0}^{L-1}h_{kl}(n)x_{kn}(i-l)+w_n(i) \tag{3}$$

where K is the number of active users and $w_n(i)$ is an additive white Gaussian noise (AWGN) sample with zero mean.

At the receiver, first the cyclic prefix is removed, then a discrete Fourier transform (DFT) is performed (with the fast Fourier transform, FFT, algorithm) to demodulate the received signal block (the entire OFDMA symbol). The post-DFT signal is

$$Y_n(m)=X_{kn}(m)H_{kn}(m)+W_n(m) \tag{4}$$

where $W_n(m)$ is the complex Gaussian noise sample with variance N_0 W/Hz, and $H_{kn}(m)$ is the complex channel frequency response of user k on subcarrier m at the nth OFDMA symbol. This frequency response can be expressed by the following equation:

$$H_{kn}(m)=\sum_{l=0}^{L-1}h_{kn}(l)e^{j2\pi lm/N}. \tag{5}$$

We use $\hat{H}_{kn}(m)$ to represent the receiver's *estimate* of channel fading $H_{kn}(m)$. Then, the estimated transmitted QAM symbol of the kth user on the mth subcarrier for the nth OFDMA symbol, denoted $\hat{X}_{kn}(m)$, is selected as the element in the signal constellation with the minimum Euclidean distance to the "channel equalized" sample. The channel equalized sample is given by

$$\hat{Y}_n(m)=Y_n(m)/\hat{H}_{k,n}(m) \tag{6}$$

and the estimated transmitted data symbol is then

$$\hat{X}_{kn}(m)=\min_{0\le q<M}|S_q-\hat{Y}_n(m)| \tag{7}$$

where S_q is the qth element in the QAM constellation, and M is the QAM constellation size. The demodulated data is then passed through the deinterleaver and decoder, to yield the final user data estimates.

3.2 Considerations for Airport Surface Area Operation of 802.16

Any OFDM modulation scheme is designed to operate well when orthogonality is maintained between the multiple subcarriers. In general this can be achieved when there is no "intersubcarrier interference," which is generally caused by Doppler spreading induced by the time variations in the transmission channel, or imperfect frequency synchronization. Multipath dispersion can also induce intersubcarrier interference, and for such dispersive channels, maintaining inter-subcarrier orthogonality requires that a guard time, known in the standard as a cyclic prefix (CP), be inserted into the transmitted signal after the data is modulated onto each subcarrier. The length of the CP in time should be longer than that of the maximum expected channel delay spread T_M [10]. We thus use our measured channel data to derive the required CP length for the various channel environments. As we noted in [2], for the worst-case, large airport NLOS regions, the CP should be at least 4-5 microseconds. Smaller CP durations can be used, particularly for LOS and NLOS-S conditions [8], but the 4-5 microsecond value can account for the worst case; this would enable a common 802.16 configuration for all regions of airports of all sizes. The cost of this common long CP is reduced efficiency (lower throughput) for the less dispersive channel regions, but the benefit is simplicity in deployment. As we will describe, this 4-5 microsecond CP value is overly conservative, and will not be recommended.

In addition, since most platforms are mobile, the channel will be time varying. Even if the platforms are temporarily non-mobile, scattering from moving objects in the environment will render the channel time variant. As previously noted, the standard does not specify all receiver processing, and one of the most important receiver processing algorithms is channel estimation. This estimation is required to compensate for channel fading that may be different on each of the transmitted subcarriers. This compensation can be viewed as equalization in the frequency domain, and has been described mathematically in the previous section (see eq. (6)). In order to enable receivers to accomplish this equalization effectively, known pilot symbols are inserted into the transmitted data. These pilot symbols should appear frequently enough to estimate the channel before it changes significantly, and should also be distributed closely enough in frequency to adequately sample the channel's fading across frequency. The standard specifies the distribution of these pilot symbols in both time and frequency, with some options. In quantitative terms, in order to accurately estimate the channel's time variation, we require multiple pilot symbols to be received within the channel's coherence time t_c. The coherence time is a statistical measure of approximately how long the channel can be assumed nearly constant [8], and this value is roughly equal to the reciprocal of the Doppler spread f_D [11]. For examples, if the airport surface relative platform velocity is approximately 26 miles/hour, at a frequency of 5 GHz, $f_D \cong 200$ Hz, which yields a coherence time of $t_c \cong 5$ milliseconds. For a velocity of 100 miles/hour, $f_D \cong 745$ Hz, and the coherence time is $t_c \cong 1.3$ milliseconds.

As previously noted, the CP duration allows a tradeoff between the multipath resistance and spectral efficiency: for a given OFDM symbol time, a longer CP means a smaller portion of the symbol time is allocated to user data, but a longer CP means that a more dispersive channel can be accommodated without destroying the inter-subcarrier orthogonality. In the 802.16

standard, the user data portion of the symbol time is denoted the "useful symbol time," T_b, with units of seconds. The CP can be one of four values, specified as fractions of T_b. These values (called the "CP ratio") are 1/32, 1/16, 1/8, and 1/4. These ratios are given the parameter name G (for "guard" time), so that the total OFDMA symbol period, called the "basic symbol period," in seconds, is $T_s=T_b(1+G)$. The standard is flexible enough so that different FFT sizes can have the same actual CP duration, but different ratios G.

The FFT size is denoted N, and this is the maximum total number of subcarriers. This value also affects the actual CP time, and so is another parameter that must be selected according to channel parameters. In summary, we repeat the two basic rules for CP selection from [2]:

1. select $T_bG>T_M$, the maximum expected channel delay spread, so that channel dispersion is circumvented by the CP;
2. select t_c/T_s as large as possible, or equivalently, T_s as small as possible, so that multiple pilot symbols are sent and received before the channel changes appreciably. .

The second rule requires that $T_s=T_b+T_bG$ is small, but the first rule requires T_bG be large, so herein lies the compromise between spectral efficiency and channel estimation accuracy.

As in our prior work, and as stated for channelization of the E-MLS band, we explore ASA performance of 802.16 with a channel bandwidth of approximately 10 MHz. In the standard, this corresponds to a "nominal channel bandwidth" of 8.75 MHz, which yields a sampling frequency of f_s=10 MHz. Depending upon filtering and adjacent channel interference requirements, this nominal 8.75 MHz channel could be allocated to a 10 MHz frequency slot. Future work could easily explore performance of 802.16 deployed with other values of channel bandwidth, e.g., 5 MHz, 1.25 MHz.

The interim report [2] explored various values for the number of subcarriers N and the CP duration, assuming various Doppler spreads (corresponding to various values of maximum ASA vehicle velocity). We refer the reader to that report for more in-depth treatment, but do provide here an example description of the calculation of throughput.

The maximum data rates achievable with any set of system parameters (N, CP, T_M, f_D) depend upon the modulation type, the rate of the FEC code r, the number of "used" subcarriers (N_{used}), and the percentage of pilot symbols. The relation $N_{used}<N$ always holds, because some subcarriers are always omitted to avoid DC offset and some are omitted for guard bands at the upper and lower limits of the signal spectrum. The value of N_{used} also depends upon the permutation, and also upon the direction of transmission (uplink or downlink).

As an example, with a particular scheme (partial usage of sub channels, PUSC) in the downlink, with N=512 subcarriers, the standard specifies N_{used}=420, where the used subcarriers include N_{data}=360 data subcarriers and N_{pilot}=60 pilot subcarriers. Thus, 92 subcarriers are *un*used, or omitted, with nothing transmitted on them. To compute the data rate in bits per second (bps), we use the relation that we transmit a maximum of N_{data} symbols (across the subcarriers) during the OFDMA symbol time of T_s seconds. We then multiply N_{data}/T_s by the number of bits per modulation symbol m, to obtain the data rate R_b bps. For example, with N_{data}=360 subcarriers and T_s=52.8 microsec, we obtain N_{data}/T_s=6.8182 Msymbols/second. If 16-QAM is used, m=4 bits per symbol yields R_b=27.273 Mbps in the 10 MHz channel, whereas if 64-QAM is used, m=6 bits per symbol yields R_b=40.909 Mbps, and if QPSK is used (m=2), we obtain R_b=13.636 Mbps. Finally, we note that this data rate does not include FEC coding, which reduces the actual user data rate to $R_{bu}=rR_b$, with $r<1$ the FEC code rate. Values for r include 1/2, 2/3, 3/4, and 5/6. The value of T_s in this example pertains to a multipath delay spread T_M=1.3 microsec, and Doppler spread f_D=286 Hz, corresponding to a velocity of 60 km/hr. Note

that these computations only compute the total data rates; data rates for individual users will be less than these values if multiple users are transmitting simultaneously.

Table 1 (augmented from Table 3 of [2]) shows a listing of various parameters for the large airport, NLOS channel for which the delay spread and Doppler spread of the previous paragraph apply. The column headed with N=512 is highlighted as a preferred choice. The last row of Table 1 specifies the parameter we denote M, which is the number of OFDMA symbols transmitted within the channel's coherence time t_c. The relation between M and the actual number of pilot symbols depends on which option is selected from the standard, and which link (uplink or downlink) is considered. Again we observe that as N increases and the CP ratio G decreases (increasing spectral efficiency), the value of M decreases, yielding fewer pilot symbols for channel estimation. Thus we trade channel estimation accuracy (which gets better as M increases) for spectral efficiency (which gets smaller as M increases).

We state again that the FFT size N=512 is a good parameter choice for the ASA, since we obtain a reasonably large value of M for good channel estimation accuracy, and still meet the CP requirement with a relatively small ratio of guard time to data symbol time. Our simulation results support this choice. In Table 1, the smaller FFT size N=128 yields a larger value of M than that for N=512, but requires a much longer CP, which substantially reduces spectral efficiency. In addition, with a smaller number of subcarriers (128 instead of 512), each subcarrier's bandwidth is four times larger, thus channel fading can be more frequency selective with respect to the subcarrier bandwidth (see Figure 3 of [2]). This can make the channel equalization described in the previous section less effective. As we noted in [2], the most conservative design choices would simultaneously allow for the largest velocity *and* the largest delay spread. Since these conditions will almost never occur simultaneously on the airport surface[1], we contend that designing for a smaller velocity and larger delay spread is a good choice for the 802.16 ASA configuration.

Table 1. 802.16 system parameters for NLOS region of large airport, with T_M=1.3 μs, v=60 km/hour, f_D=286 Hz.

FFT size N	128	512	1024	2048
N_{data}	72	360	720	1440
N_{pilot}	12	60	120	240
CP ratio G	1/8	1/32	1/32	1/32
CP period T_g (μs)	1.6	1.6	3.2	6.4
Useful OFDMA Symbol Period T_b (μs)	12.8	51.2	102.4	204.8
OFDMA Symbol Period T_s (μs)	14.4	52.8	105.6	211.2
M=floor(t_c/Ts)	242	66	33	16

[1] The largest possible velocities apply to aircraft taking off or landing, or for ground vehicles traveling in open areas. In these cases, since the channel will nearly always be LOS, channel dispersion (T_M) is minimal [8].

In the previous report, we devoted some time to discussion of the channel model itself. We refer the reader to that report, and to [8], for additional background and exhaustive detail, with models for all regions of all airport sizes, with options for trading model fidelity and complexity. In this report we do provide one channel model explicitly. Some of this material also appears in [12].

The physical wireless ASA channel is modeled as a time varying linear filter. The most commonly used model for such complex wireless channels is the tapped-delay line model [13], illustrated in Figure 3. In this figure, the x's denote channel input symbols and the y's the channel output symbols. The τ's are delays, referenced to the first-arriving multipath component, and the h's are the channel impulse response (CIR) random amplitudes, specified in the complex baseband CIR equation as follows:

$$h(t) = \sum_{i=0}^{L-1} z_i(t)\alpha_i(t)e^{j\phi_i(t)} = \sum_{i=0}^{L-1} h_i(t) \tag{8}$$

where i denotes the channel tap (~multipath component) index, the z's are the tap "persistence" random processes, with $z_i(t) \in \{0,1\}$, the α's are the randomly fading amplitudes, and the ϕ's are the random phases. The number of taps in the tapped delay line model is L. Note that the values of the delays depend on the channel bandwidth employed: for our 10 MHz channel, the value of delay difference $\Delta\tau = \tau_{i+1} - \tau_i$, is the reciprocal of this, or $\Delta\tau$=100 nanosec.

The persistence processes $z(t)$ are used to model the finite "lifetime" of the multiple propagation paths. Specifically, due to the dynamic nature of the channel, the multipath components can be modeled using a "birth/death" (i.e., on/off) process. The tap persistence processes are modeled using two-state first-order Markov chains, one such chain for each of the taps. State 1 denotes the presence of multipath at a given value of delay, and state 0 signifies the absence of multipath. The Markov chain is specified by two matrices, the transition *(TS)* matrix and the steady state *(SS)* matrix, defined as follows,

$$TS = \begin{bmatrix} P_{00} & P_{01} \\ P_{10} & P_{11} \end{bmatrix}, \quad SS = \begin{bmatrix} P_0 \\ P_1 \end{bmatrix}. \tag{9}$$

The element P_{ij} in matrix TS is defined as the probability of going from state i to state j. Each SS element P_j gives the steady state probability associated with the j^{th} state, roughly corresponding to the long term fraction of time the multipath component is in that state. Worth mentioning is that incorporation of the persistence processes into the channel model renders the channel statistically *non*-stationary, in contrast to most common models. This adds to the model complexity, but provides greater realism.

We model the tap amplitudes using the Weibull probability distribution [14]. The rationale behind the use of this distribution is provided in [8], but its use is not uncommon, e.g., [15]. The Weibull model offers substantial flexibility, as it has two parameters, a and β,

$$p_W(x) = \left(\beta / a^{\beta}\right) x^{\beta-1} \exp\left(-\left(x/a\right)^{\beta}\right), \tag{10}$$

where $\beta>0$ is a shape factor that determines fading severity, $a=\sqrt{E(w^2)/\Gamma[(2/\beta)+1]}$ is a scale parameter, and Γ is the gamma function. A value of $\beta=2$ yields the well-known Rayleigh distribution, and $\beta<2$ implies more severe fading.

Table 2 provides the parameters that specify our most accurate 10 MHz channel model for the NLOS region of a large airport. This "high fidelity" model is denoted M2, to distinguish it from two alternative channel models, M1 and M3 (see [8] for detailed specifications of other models). Since we also model correlation between the channel taps (scattering is often correlated, in contrast to common models, e.g., [13]), to complete specification of this channel model also requires a 50×50 matrix for its correlation coefficients, which we do not provide here. Note also that the remaining persistence parameters can be obtained from those in the table by the following relations: $P_{0,k}=1-P_{1,k}$; $P_{01,k}=1-P_{00,k}$; and $P_{10,k}=1-P_{11,k}$. In [8] we developed several models with varying levels of complexity and fidelity (i.e., M1, M2, and M3). In this report's section on simulation results, we provide some additional explication on this.

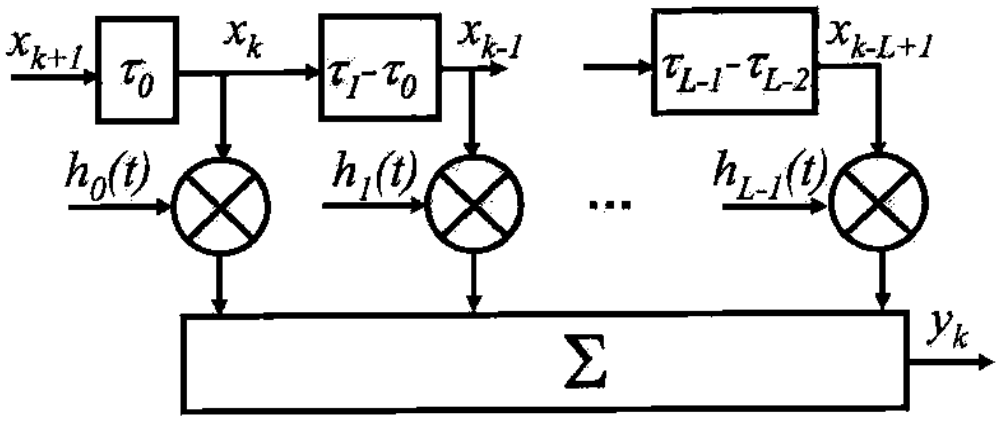

Figure 3. Tapped delay line model for ASA wireless channel.

Table 2. Channel fading amplitude and persistence parameters for most accurate 10 MHz, NLOS, large airport model [8].

Tap Index k	Energy	λ_k	K_k	P_{0k}	P_{1k}
1	0.0111	1.3908	0.1747	0.9008	0.5316
2	0.0855	1.3400	0.9969	0	0.9969
3	0.1055	1.2700	1	*NA*	*NA*
4	0.0678	1.3800	0.9102	0.1970	0.9207
5	0.0457	1.4900	0.8642	0.2506	0.8822
6	0.0384	1.5900	0.8307	0.3246	0.8623
7	0.0296	1.3971	0.8036	0.3440	0.8397
8	0.0254	1.4382	0.7871	0.3437	0.8227
9	0.0227	1.4711	0.7626	0.3785	0.8065
10	0.0199	1.5432	0.7495	0.3961	0.7984
11	0.0188	1.5092	0.7388	0.4137	0.7929
12	0.0176	1.5794	0.7414	0.4007	0.7909
13	0.0165	1.6293	0.7184	0.4383	0.7800
14	0.0163	1.6234	0.7194	0.4378	0.7807
15	0.0152	1.6252	0.7150	0.4478	0.7801
16	0.0144	1.6905	0.7082	0.4533	0.7749
17	0.0148	1.6966	0.7158	0.4281	0.7732
18	0.0139	1.7364	0.7043	0.4304	0.7610
19	0.0145	1.6180	0.7014	0.4524	0.7670
20	0.0137	1.7258	0.7032	0.4392	0.7636
21	0.0138	1.7800	0.6976	0.4654	0.7685
22	0.0132	1.7217	0.6954	0.4469	0.7580
23	0.0135	1.7212	0.6951	0.4442	0.7564
24	0.0127	1.7690	0.6920	0.4547	0.7575
25	0.0124	1.7380	0.6854	0.4613	0.7529
26	0.0123	1.7383	0.6810	0.4600	0.7471
27	0.0127	1.8041	0.6917	0.4691	0.7635
28	0.0128	1.7438	0.6850	0.4665	0.7548
29	0.0127	1.7778	0.6925	0.4400	0.7515
30	0.0127	1.7662	0.6895	0.4526	0.7536
31	0.0127	1.7794	0.6956	0.4402	0.7549
32	0.0125	1.7533	0.6961	0.4423	0.7567
33	0.0126	1.7548	0.7051	0.4212	0.7579
34	0.0122	1.7416	0.6915	0.4674	0.7625
35	0.0128	1.7467	0.6803	0.4588	0.7458
36	0.0129	1.7158	0.6907	0.4631	0.7597
37	0.0129	1.7144	0.6827	0.4558	0.7472
38	0.0134	1.7142	0.6874	0.4491	0.7497
39	0.0131	1.7238	0.6915	0.4793	0.7679
40	0.0126	1.7846	0.6840	0.4550	0.7484
41	0.0124	1.7431	0.6827	0.4456	0.7425
42	0.0127	1.6913	0.6774	0.4657	0.7457
43	0.0128	1.6938	0.6878	0.4627	0.7562
44	0.0130	1.7356	0.6861	0.4499	0.7484
45	0.0129	1.7044	0.6937	0.4406	0.7532
46	0.0142	1.5515	0.7082	0.4230	0.7624
47	0.0145	1.5250	0.6939	0.4425	0.7542
48	0.0142	1.5565	0.6946	0.4264	0.7477
49	0.0145	1.5858	0.7141	0.4187	0.7675
50	0.0147	1.5480	0.7004	0.4128	0.7490

4. Brief Observations from Recent Literature

The 802.16 standard is seeing an enormous amount of attention in the research and development community. Much work has been, and is still being done, on generic OFDM and OFDMA transmission and reception in multiple environments, and this can pertain to any of the existing or developing standards, e.g., 802.11a, 802.16, 802.15, etc. Herein we do not aim to review all this work, but instead focus on a few issues of interest in work specifically aimed at the 802.16 standards.

Reference [16] is a recent paper that explores the use of 802.16 by a large community with demanding requirements—the US military. This paper provides an overview of some of the MAC and PHY features of the standard, and describes how the BS determines all transmission characteristics of all active links in centralized (PMP) applications. It also describes the multiple QoS parameters that must be considered in service provisioning. One of the most promising potential military uses of 802.16 is stated as its capability to offer a high-capacity, long-range, wireless "backbone" service. This requires directional antennas. Use of 802.16 in mobile ad-hoc networks (MANETs) is also briefly described. A limitation of 802.16 discussed in [16] is range: without directional antennas, a range of only 40-100 meters in cluttered environments may be possible if high data rates (>50 Mbps) are desired. Another limitation is that mobility is likely limited to velocities of less than 90 mph, which should not pose a problem for ASA applications unless takeoff/landing connectivity is required.

Two other recent papers describe another potential limitation of 802.16—its security in the presence of PHY and higher-layer disruptions. The authors of [17] describe the performance of 802.16 in the presence of two types of intentional interference, or jamming: a wideband noise jammer and a multiple tone jammer. They show that the 802.16 system is quite vulnerable to jamming of both types, and that severe throughput reductions result from even moderate power jammers. The multiple tone jammer is very effective at degrading performance, particularly when the tones jam those subcarriers that contain the pilot symbols, thus interfering with the system's ability to perform accurate channel estimation and compensation. This is true of OFDM systems in general, and is something we have also investigated [18]. Although the 802.16 adaptive modulation, coding, and interleaving can aid in maintaining link connectivity in the presence of jamming, multiple tone jamming of pilots can easily reduce throughput by 90% or more, even when the total jammer power is 10 dB below that of the received signal power. Designing an adaptive pilot distribution algorithm could substantially improve this, but would require some modification to the standard.

Reference [19] discusses the security of 802.16 when used in mesh mode, but some results also apply to the standard "centralized," or point-to-multipoint mode. In particular, the authors describe how the system performance can relatively easily be degraded by spoofing attacks by unauthorized SSs. This paper also provides some additional references that describe other vulnerabilities of 802.16. These would be worth investigation for future work.

Finally here, we cite [20], which provides results for propagation path loss for the 3.5 GHz band in which 802.16 is likely to be widely deployed. The authors found that for suburban and campus-like environments, the measured path loss exponent was approximately 3-3.5. This is larger than that found for the NLOS-S ASA environment at 5 GHz, but could be representative of that in NLOS ASA conditions.

5. Example Simulation Results

In this section we provide some new computer simulation results. These results extend those in [2], and again apply to both the PHY and MAC layers.

5.1 PHY Performance Results

A high-level block diagram of the basic system, as simulated, is illustrated in Figure 4. This can be viewed as a diagram that encapsulates the transmission and reception systems shown in Figures 1 and 2, and also includes the wireless channel. The various system inputs and key parameters are indicated in Figure 4. All simulations were conducted in Matlab®. We simulated the PHY layer of 802.16e, both with and without FEC encoding and decoding, to assess performance on the airport surface channel.

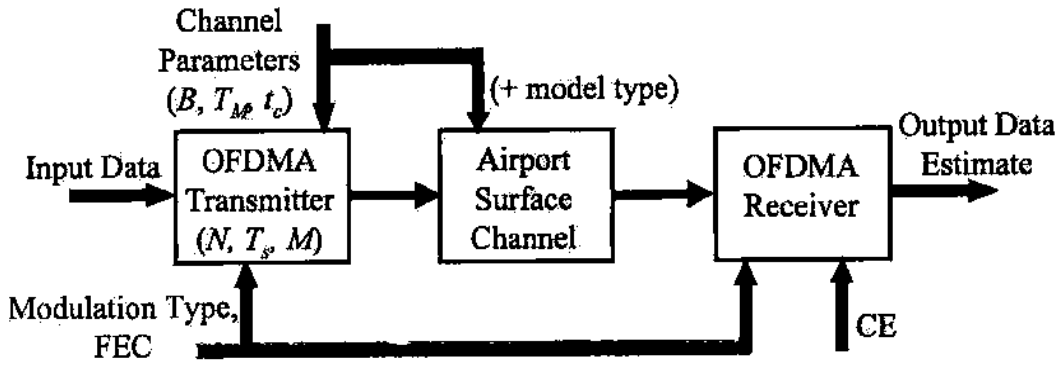

Figure 4. Basic 802.16 simulation configuration.

5.1.1 BER Performance over Multiple Channel Types

In this section we show BER performance results similar to those provided in [2], but for airports of all three sizes (large, medium, and small). Modulation and FEC are of the same types as that discussed in [2].

The 802.16e standard has defined different subcarrier permutations for the uplink and downlink. In this section we focus on the uplink PUSC, in which each subchannel is composed of six "tiles" (defined subsequently) chosen by a random permutation, and each active user is assigned one or more subchannels. For the uplink PUSC, among the N=512 subcarriers, the leftmost 52 subcarriers and the rightmost 51 subcarriers are (unused) guard subcarriers. With the central DC subcarriers excluded, there are 408 subcarriers available for data and pilot transmission. Worth noting is that although the downlink configuration differs from that of the uplink, results for the downlink will be largely similar to those for the uplink, as seen in [2].

For the uplink PUSC, each subchannel consists of six tiles chosen by the random permutation. The positions of pilots and data symbols are shown in the tile structure in Figure 5. The horizontal axis denoted "subcarrier index" corresponds to frequency, in units of subcarrier frequency separation in Hz, and the vertical axis, labeled "time," is in units of the OFDMA

symbol time T_s. As illustrated, within this tile are 12 symbols, 4 of which are dedicated to pilot symbol transmission, hence the relative throughput for this tile is 8/12, or 2/3.

There are many different channel estimation (CE) algorithms available in the literature. The optimum estimation algorithm is a 2-D Wiener filter, but this is computationally expensive, and requires we know the channel statistics exactly. This 2-D filter operates in the time and frequency domains jointly. Sub-optimum estimation has lower computational complexity by separating the time and frequency estimation algorithms, and this is what we employ.

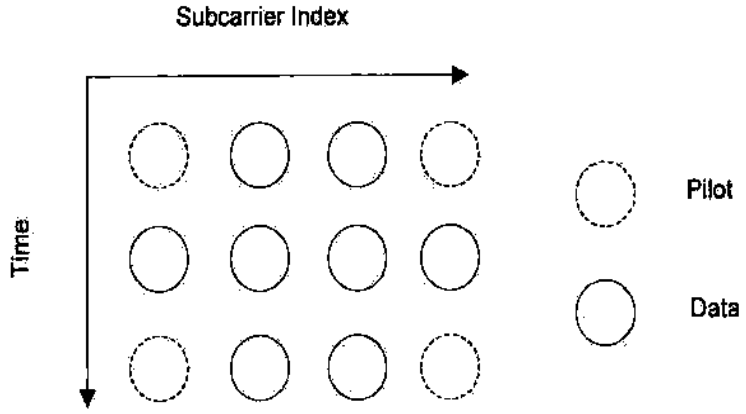

Figure 5. Illustration of 802.16e "tile" structure for uplink PUSC.

We have investigated three simplified CE methods using averaging and linear interpolation techniques that allow us to obtain good tradeoffs between channel estimation accuracy and computational complexity. These estimation algorithms are as follows:

i) CE 1 uses an average of the pilot symbols in the time and frequency domains to obtain the channel estimates. CE 1 applies to the case where the channel coherence time is much larger than the tile duration, so fading on the three OFDMA symbols can be modeled as a constant, and the averaging reduces the noise in the estimates; CE 1 also requires that fading varies little over four adjacent subcarriers in the same tile.

ii) CE 2 uses an average of pilot symbols in the time domain and linear interpolation in the frequency domain to estimate channel fading on data subcarriers. Like CE 1, CE 2 applies to the case where the channel coherence time is much larger than the tile duration. Different from CE 1, in the frequency domain, CE 2 assumes that fading amplitudes over four adjacent subcarriers in a tile structure can be well approximated as a linear function of frequency.

iii) CE 3 uses linear interpolation of the pilot symbols in both time and frequency domains to obtain the channel fading estimates on data subcarriers. In the time domain, CE 3 applies to the case where the fading amplitude values over three OFDMA symbol durations in the tile are linearly related. Similar to CE 2, in the frequency domain CE 3 assumes that fading over four adjacent subcarriers in a tile structure is also well approximated as linear in frequency.

All our simulations in this section use the uplink PUSC permutation in the frequency domain and random subchannel scheduling in the time domain. Results in [2] showed that generally, performance was best when both the time and frequency domain permutations are used. Modulation is 16-QAM and unity average channel gain is assumed on each subcarrier (this

corresponds to neglecting large scale fading (e.g., very slow "shadowing") and path loss, which can be accommodated by proper link budgeting and power control). All simulations conducted in Matlab® use the system parameters shown in Table 1. For simplicity, initially we only investigate system performance with/without the mandatory convolutional code of rate r=1/2, constraint length 7 (memory 6, with generator vectors $\mathbf{g}_1=(171)_8$, $\mathbf{g}_2=(133)_8$). Hard decision Viterbi decoding is performed using Matlab's built-in convolutional encoding/decoding routines. Interleaving is performed according to the specification in the 802.16e standard. The maximum Doppler frequency is assumed to be ~300 Hz, which corresponds to a maximum relative velocity of 40 mph on the airport surface.

Figure 6 compares the coded/uncoded BER performance versus bit energy to noise density ratio E_b/N_0 (roughly the signal to noise ratio, SNR) of 802.16 using the M2 channel model for large airports, for the different channel estimator schemes discussed above. Channel estimators 2 and 3 have similar BER performance, which is worse than the perfect estimation case, as expected. Channel estimator 1 performs very poorly in this case. A BER (P_b) of 3×10^{-3} at E_b/N_0=21 dB with perfect channel estimation highlights the degradation due to the severe frequency selectivity and fading of the large airport channel—for comparison, on a non-fading AWGN channel, uncoded 16 QAM attains this BER at approximately E_b/N_0=11 dB, and has a BER below 10^{-9} at E_b/N_0=17 dB.

Figure 7 compares the coded/uncoded BER performance of 802.16 using the simpler M1 channel models for different airports. The M1 models include channel tap persistence and correlated Weibull fading, but have fewer taps than those of the M2 models. For example, for the large airport, the M1 model has only 14 taps, whereas the M2 model has 50 taps. Generally, in all our simulations, over all conditions, the large airport performance is the worst, followed by that on the medium airport channel, with the small airport channel performance being best. As noted in [8], this is expected, as the channels go from most to least dispersive as we go from large, to medium, to small airports. Although Figure 7 shows results for the M1 channel models, similar trends appear for the other model types.

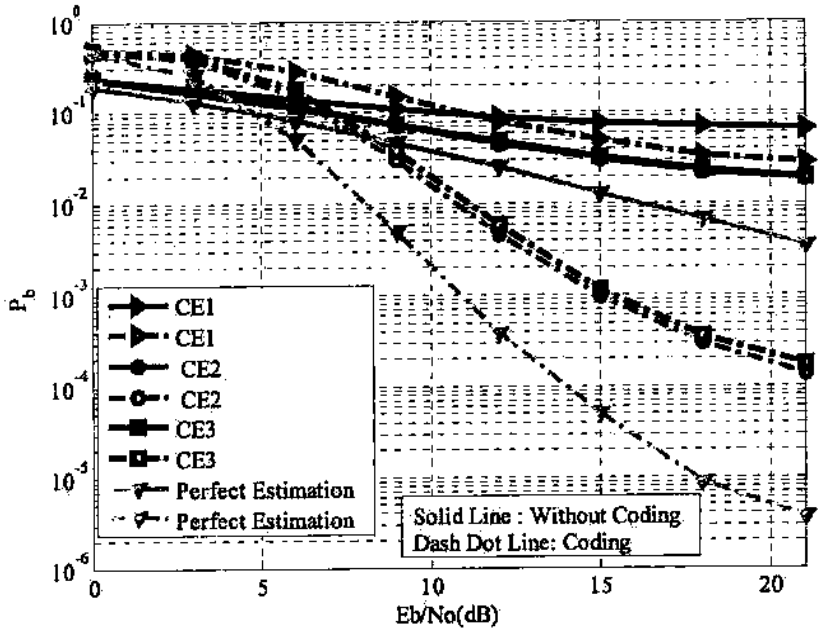

Figure 6. BER vs. E_b/N_0 for large airport M2 channel, N=512, uplink PUSC, active user number K=5, f_D=300 Hz.

We also point out that in these figures, for large and medium airports, the models are for NLOS regions, and for small airports, the models are based on NLOS-S regions, as small airport channels are best classified as having only the two regions, NLOS-S and LOS [8]. For clarity, the performance of only the best possible channel estimator is shown in Figure 7. The BER performance for the NLOS-S region of the small airport with perfect channel estimation acts as a lower bound for both coded and uncoded cases. As we would expect, the BER performance in Figure 7 with actual channel estimation is worse than that of perfect estimation. As noted previously, channel model M2 provides the most accurate representation of the channel, but is more complex to implement than M1.

Figure 8 provides a similar coded/uncoded BER performance plot for the 802.16 system using the M2 models for airports of different sizes. For clarity, the performance of only the best possible channel estimator is shown in this figure. Again the BER performance for the small airport NLOS-S region using perfect channel estimation acts as a lower bound for both coded and uncoded cases. As expected, the BER performance degrades from that in Figure 7 due to the more dispersive Model-2 channel. For example, with an SNR of 10 dB, on the large airport, M1 yields a BER of roughly 10^{-3} in Figure 7, whereas the BER is approximately 10^{-2} for the M2 channel in Figure 8 at the same value of SNR. We also note that there is a significant difference between the BER performance obtained using actual channel estimation techniques and perfect channel estimation for all airports. This indicates that more sophisticated channel estimation schemes may be worth investigation for the performance improvement they can provide.

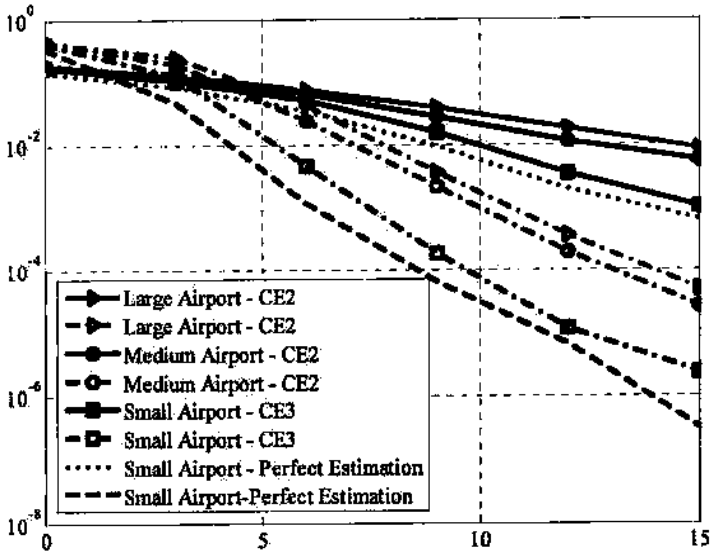

Figure 7. BER vs. E_b/N_0 for all airports, M1 channel, N=512, uplink PUSC, active user number K=5, f_D=300 Hz, best channel estimation techniques.

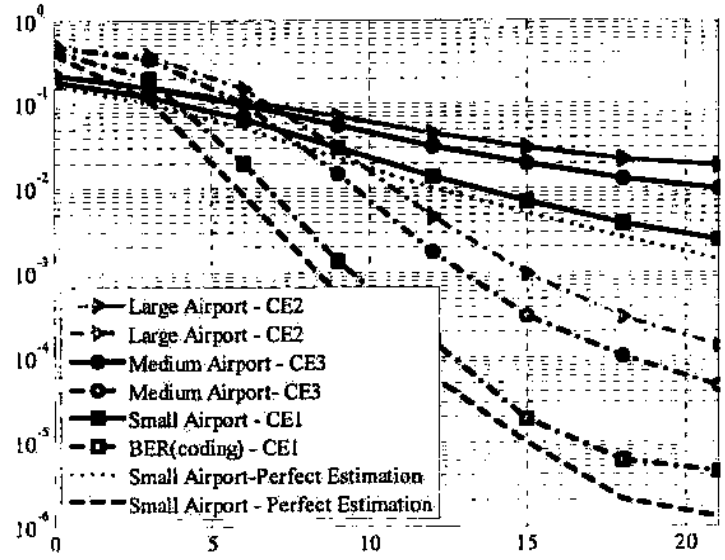

Figure 8. BER vs. E_b/N_0 for all airports, M2 channel, N=512, uplink PUSC, active user number K=5, f_D=300 Hz, best channel estimation techniques.

5.1.2 BER Performance for Large Airport Channel, New FEC & Jamming

In this section we provide BER performance results for transmission on the worst-case, large airport NLOS channel, using the same 802.16e system parameters as in the previous

section, but with some different conditions. The first condition is the use of a newer, more powerful, FEC code, and the second condition is performance in the presence of intentional interference, or jamming.

Specifically, the new code is a "turbo" code, which uses multiple constituent convolutional encoders and an interleaver at the transmitter, and multiple iterative decoders at the receiver [21]. This code has rate r=1/2, with generator matrices $\mathbf{g}_1$=$\mathbf{g}_2$=[1 1 1 1 1;1 0 1 0 1], or [37; 25] in octal format. This code was selected based upon its good performance in comparison to other codes available in the literature. The turbo code interleaver was a random interleaver. Figure 9 shows the BER performance of this code versus SNR, along with the uncoded performance, and that of the conventional convolutional code used in the previous section. The more powerful turbo code gains several dB in performance over the conventional code for error probabilities lower than about 10^{-3}. These gains do increase somewhat as SNR increases, but then decrease at very low error rates, below about 10^{-9}; this behavior is typical of these codes. The performance in Figure 9 is for K=5 simultaneous users, and can be compared with that of the large airport plots in Figure 6 (with perfect CE). Clearly, the use of turbo coding improves performance, and is strongly recommended for all applications except possibly those with very stringent delay constraints.

The performance of 802.16 in the presence of jamming is also of interest from the perspective of system security. As noted in section 4, it is most effective for a jammer to disrupt those subcarriers that contain pilot symbols, as this degrades the channel estimates for all subcarriers. We show simulation results for pilot subcarrier jamming in Figure 10, for uncoded bit error probability.

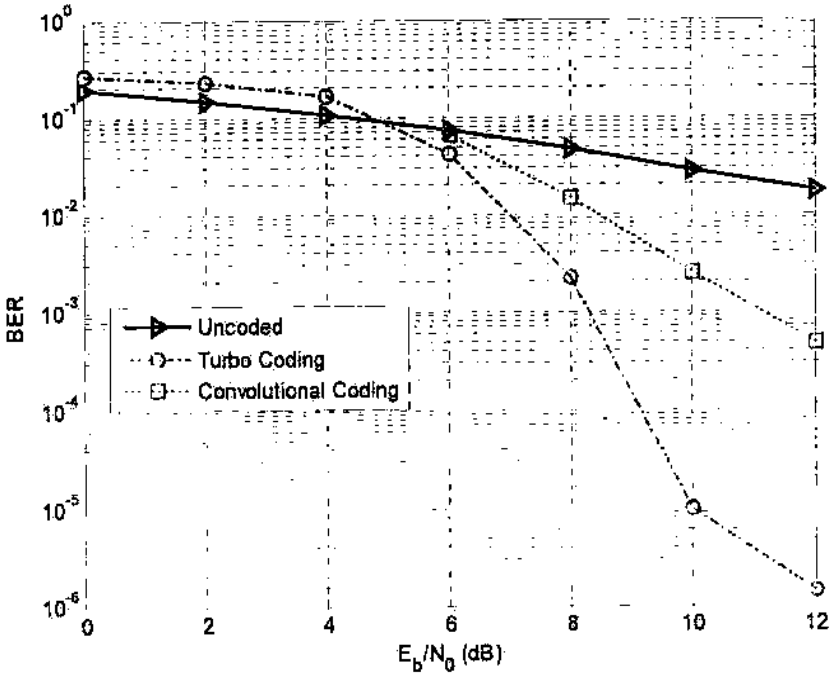

Figure 9. Coded and uncoded BER vs. E_b/N_0 for large airport NLOS M2 channel, N=512, uplink PUSC, active user number K=5, f_D=300 Hz, showing turbo coding gains.

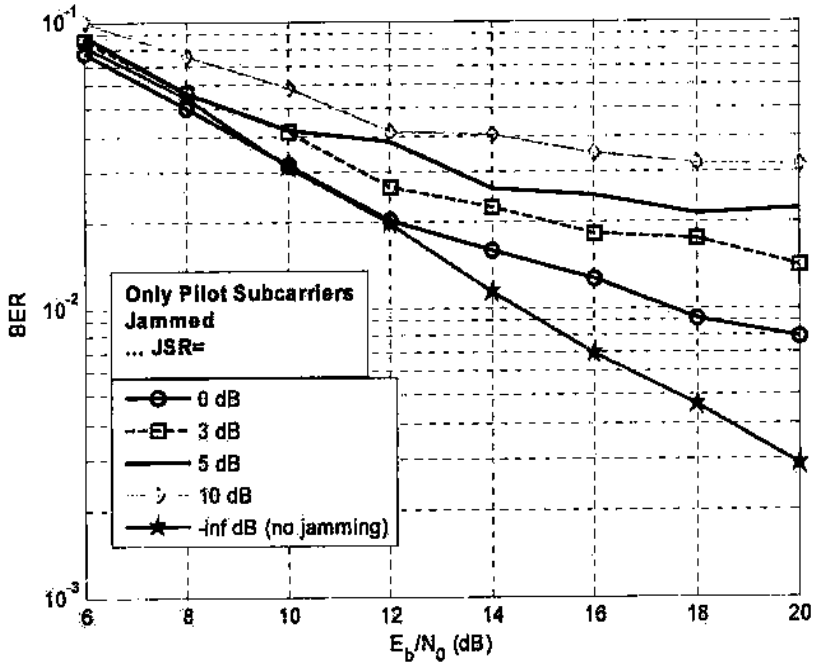

Figure 10. *Un*coded BER vs. E_b/N_0 for large airport NLOS M2 channel, N=512, uplink PUSC, active user number K=5, f_D=300 Hz, in the presence of multiple tone *pilot* jamming.

Figure 10 shows that when the pilot symbols are jammed, performance degrades significantly. The abbreviation JSR in the legend of Figure 10 stands for jammer to signal power ratio, and performance clearly degrades as JSR increases. Significant degradations (a BER "floor") in performance result for JSRs equal to or larger than 0 dB.

Figure 11 shows the corresponding coded BER performance results in the presence of multiple tone pilot jamming, using the rate-1/2 convolutional code previously described. The "roughness" of the curves is attributable to insufficient averaging, which requires long simulation run times. Nonetheless the trend is clear, and shows that coding can be useful not only to combat channel fading, but can also enhance performance in the presence of interference as well.

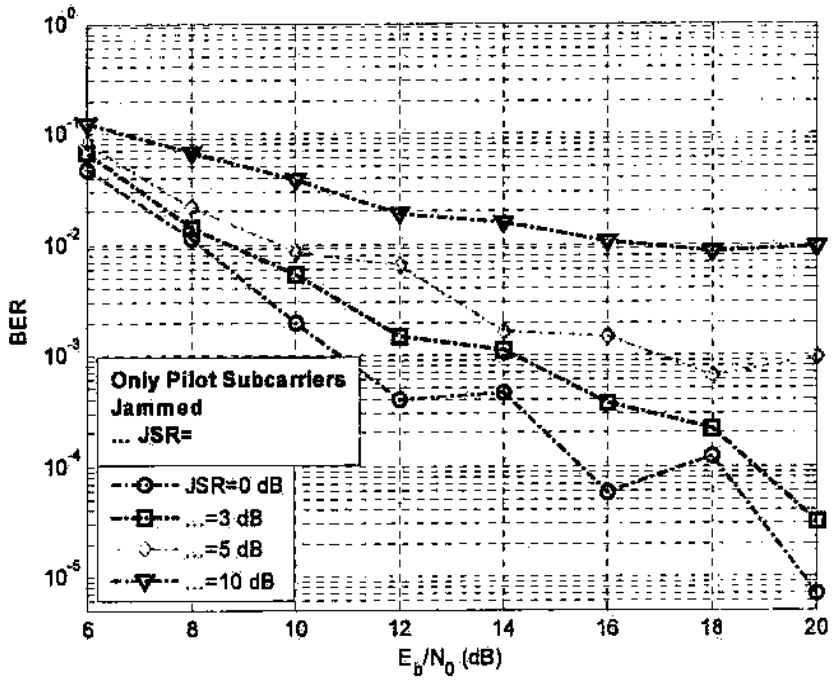

Figure 11. Convolutional *coded* BER vs. E_b/N_0 for large airport NLOS M2 channel, N=512, uplink PUSC, active user number K=5, f_D=300 Hz, in the presence of multiple tone pilot jamming.

Finally in this section, we show results when all subcarriers are jammed with tones, not only those subcarriers containing pilot symbols. This condition is easier for the jammer to create, since the jammer need not know the location in frequency of the pilot symbols. Figure 12 shows performance in this case is actually worse than the case when only pilot symbols are jammed, as seen by comparing with results in Figure 10. This can be explained by the fact that for when all subcarriers are jammed, not only is channel estimation degraded, but symbol detection for all data symbols is also degraded. Figure 13 shows analogous results for the coded case, which can be compared with the pilot-jamming-only results of Figure 11.

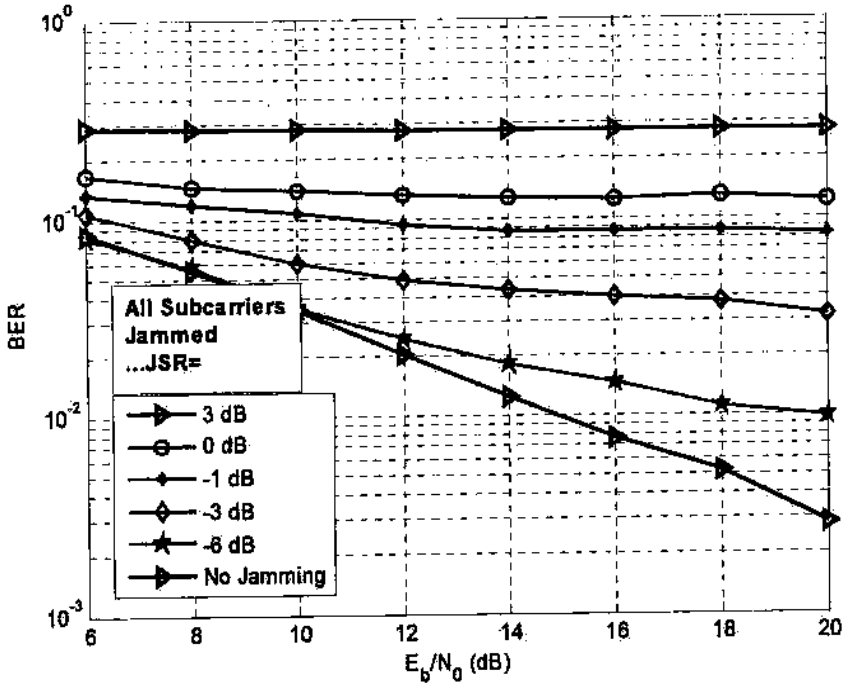

Figure 12. *Uncoded* BER vs. E_b/N_0 for large airport NLOS M2 channel, N=512, uplink PUSC, active user number K=5, f_D=300 Hz, in the presence of multiple tone jamming of all subcarriers.

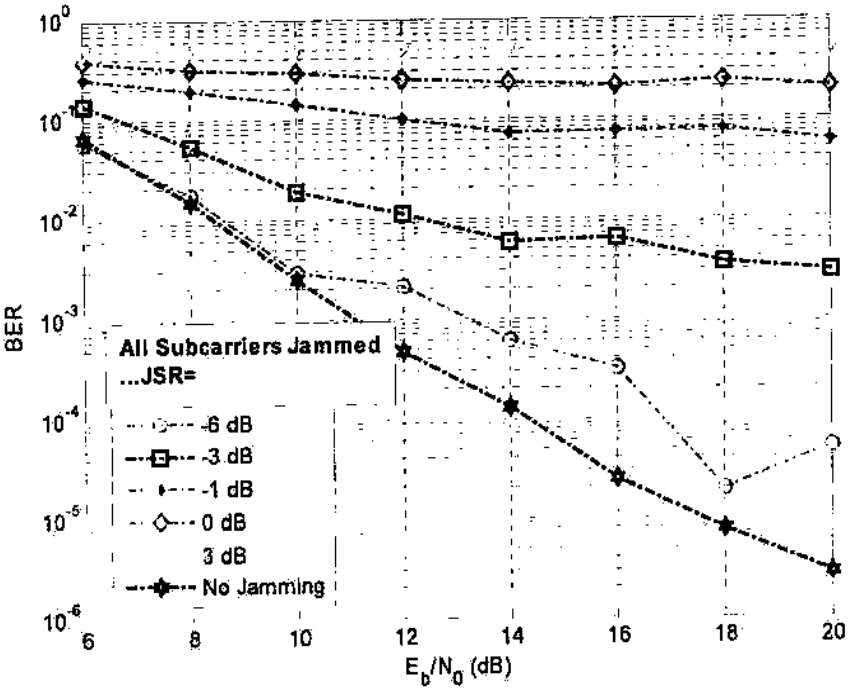

Figure 13. *Coded* BER vs. E_b/N_0 for large airport NLOS M2 channel, N=512, uplink PUSC, active user number K=5, f_D=300 Hz, in the presence of multiple tone jamming of all subcarriers.

5.2 Scheduling Performance Results

In this section, we illustrate MAC layer performance, specifically by subcarrier scheduling, aiming to maximize the throughput under QoS constraints. For these results, we configure the system as described by the parameters in Table 3, the same as that used in [2]. Here we show results for different sized airports. To keep the scheduling algorithms simple and the results easy to interpret, we keep the number of users moderate. We do though employ a more aggressive scheduling algorithm based on allocating *each* subcarrier rather than allocating according to the AMC permutation subchannel specified in the standard; this allows for finer resolution of achievable data rates, without sacrificing performance. This approach was introduced in [2], and when fading doesn't vary much in the consecutive subcarriers of each AMC subchannel, our subcarrier based allocation algorithms provide behavior similar to the AMC subchannel algorithm, but with finer data rate resolution, and ultimately, a larger potential data rate for each user. Alternatively, we can also view our aggressive scheduling results as bounds to those achievable with the AMC subchannel scheduling—specifically, the data rates we achieve with our algorithm may be viewed as upper bounds to the data rates achievable with the 802.16 standard scheduling algorithms.

For QoS, we allow two grades of service, one denoted Guaranteed Performance (GP), and the other denoted Best Effort (BE). Resource scheduling and allocation of bandwidth is done to give priority to the GP users, so that bandwidth is first allocated to these GP users, then the remaining available bandwidth is allocated to BE users according to a proportional fairness scheduling criterion. For these simulations, we also must specify the scheduling period T_{sch}. Here we choose this as 1/6 the channel coherence time, so that fading is relatively constant during the scheduling period.

Table 3. Parameters for two service classes for MAC results.

	GP User	BE User
Required BER (uncoded)	10^{-2}	10^{-2}
Required Date Rate R_b (Mbps)	2	Not Guaranteed
Number of Users	First 50%	Last 50%

The operations performed within the scheduling algorithm are subcarrier allocation and the selection of the modulation scheme for each user, during each scheduling period. We assume that channel estimation for the purpose of scheduling is perfect, and the outputs of the scheduling algorithm are then applied for the subsequent N_b OFDMA symbols. The specific scheduling algorithm is described in [2], and is not repeated here in detail. We do note that subcarriers are allocated to the GP users with the rule of "first-come, first-served" and that the modulation on each subcarrier is selected according to the rule specified in [22]. This rule works in such a way that if the simplest modulation scheme can not satisfy the GP BER requirement on that subcarrier, we leave that subcarrier unused for that particular user, and allow subsequent (BE) users to employ it, if feasible. This most often happens to the "last come" GP user in a full or over-loaded system. The remaining subcarriers are allocated to BE users according to proportional scheduling, as described in [2].

All simulations again use the (highlighted, N=512 column) 802.16e system parameters shown in Table 1, over different non-stationary airport channels. For these MAC results, we use the M2 channel models throughout since they are the most accurate representations of the underlying physical channel. The average channel gain on each subcarrier is assumed to be unity, with perfect channel estimation. Figure 14 shows the data rates vs. user index in the large airport. The first six users are GP users, whereas the latter six users are BE users. Note that the resources (subcarriers) are allocated to the BE users before the last GP user's data rate requirement is fully satisfied. This happens because channel fading on the available subcarriers of the last GP user is so bad that even the simplest modulation scheme cannot satisfy the BER requirement, so the system just allocates the available subcarriers to the BE users. It can also be seen that data rate fairness is achieved among the BE users.

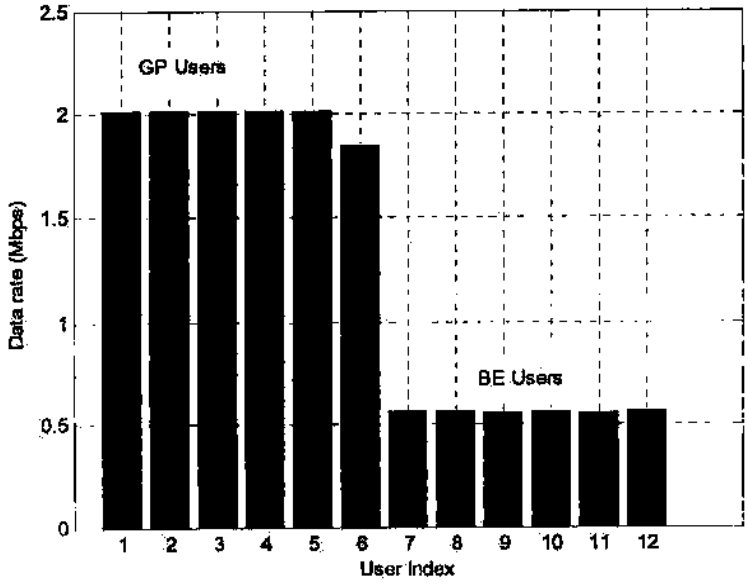

Figure 14. Date rates vs. user index in the large airport, M2 NLOS channel model, 10 MHz bandwidth.

Analogous to Figure 14, Figure 15 depicts data rates versus user index in the medium airport channel. Again the first six users are GP users and the latter six are BE users. In this airport, the data rate requirements of the GP user are fully satisfied, and the remaining subcarriers are allocated to the six BE users with fairness. One can also see that the achievable data rate of the BE users is larger than that in the large airport case, due to the better channel conditions.

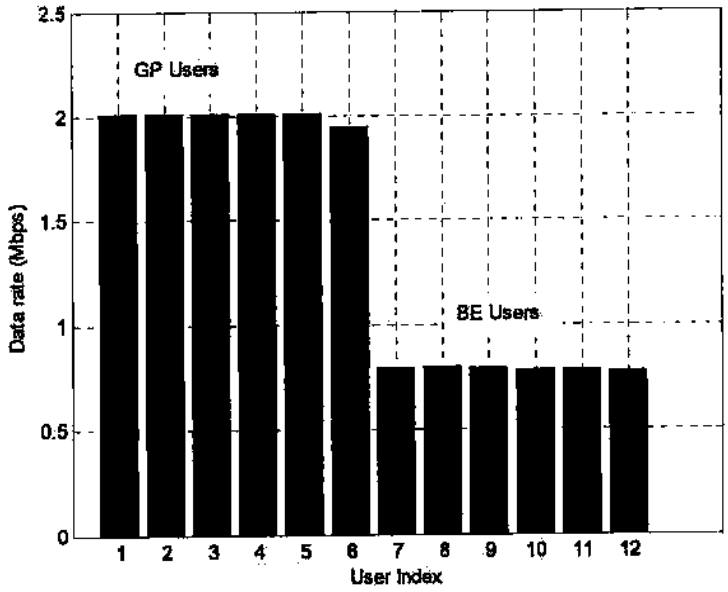

Figure 15. Date rates vs. user index in the medium airport, M2 channel model, 10 MHz bandwidth.

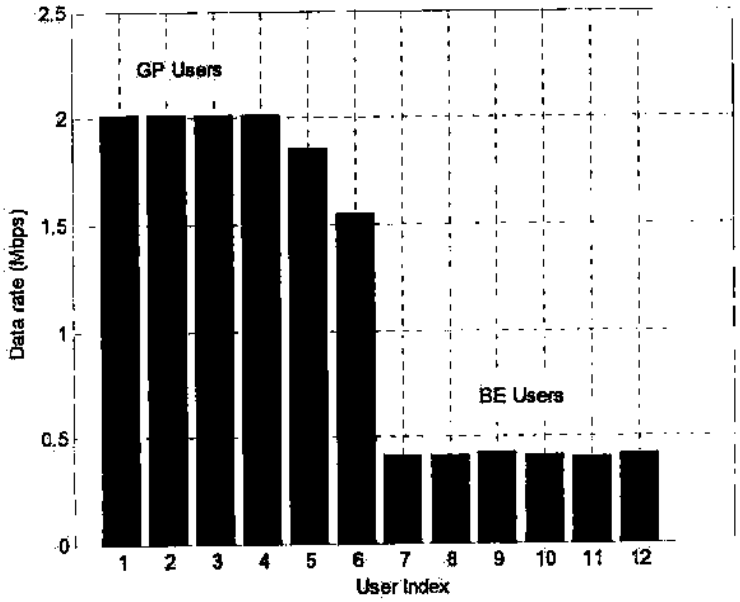

Figure 16. Date rates vs. user index in the small airport, M2 channel model, 10 MHz bandwidth.

Figure 16 shows the data rates versus user index for the small airport channel. Interestingly, scheduling performance in this channel is actually worse than that of both Figures 14 and 15. A plausible reason for this is the reduction in frequency diversity attainable in the

NLOS-S channel for the small airport. That is, due to the smaller time delay dispersion, the channel is not as frequency selective as it is in the larger airport channels, so that when fading occurs, it is likely to occur on a larger fraction of subcarriers. The subcarrier allocation algorithm we use tries to exploit frequency diversity among different subcarriers. In addition, the objective of our subcarrier allocation algorithm is not only throughput, but also fairness among the different active users. In the NLOS-S case for the small airport, there may be minimal frequency diversity that can be exploited, and the throughput of active users is more susceptible to deep broad band fades than in the other cases. The complexities and interactions among diversity, fairness, and throughput are worth further study.

6. Summary, Conclusions, and Recommendations

In summary, in this report we have provided an overview of the original project objectives, the actual work we have done, and an overview on the 802.16 wireless technologies. We provided analytical and simulation results useful for the configuration and future deployment of these technologies on the airport surface area.

For conclusions, we re-affirm that the goal of deploying 802.16 on the ASA is a feasible and very useful one. The 802.16e technologies are a flexible, efficient, and high performance set of technologies that can dramatically improve the data-carrying capacity of the ASA environment, for multiple applications. The availability of nearly 60 MHz of E-MLS band spectrum will enable a number of mobile and point-to-point data links to operate on the ASA for numerous uses.

Our analytical and simulation results show that in the worst case channel conditions, depending on QoS requirements, tens of megabits per second (Mbps) can be transferred reliably, for multiple users, when channel bandwidths of 10 MHz are used. This pertains when signal to noise ratios on the order of 15 dB are attainable. Data throughputs for larger bandwidths are at least proportionally larger, and throughputs for smaller bandwidths should approximately scale with bandwidth. Performance, in terms of error probability, for better channel conditions (e.g., for LOS cases) will be substantially better than that in the worst-case, NLOS, large airport case. Thus some of our results represent approximate worst case results.

We also showed that performance can be substantially improved with advanced coding techniques, explicitly turbo coding. The 802.16 standards allow, and have a specification for, using these codes. They deserve some further study.

In terms of the robustness to 802.16 to interference, we presented results for performance in the presence of intentional jamming. As is well known, the OFDMA schemes are *not* robust to this impairment, and this fact should be considered before deploying these systems in cases where service disruption or degradation is unacceptable. The jamming we studied is a simple form of multiple tone jamming, and can be easily implemented by an entity with minimal knowledge of system operation. Spatial diversity and the use of directional antennas can aid in improving performance in jamming.

As for recommendations, we first state that actually deploying an 802.16 system in the ASA environment is still strongly recommended. An actual testbed that contains at least one base station, and multiple subscriber stations, should be procured, configured, and thoroughly tested. Ideally this should be done in the E-MLS band, but that may not be possible in the near term without a substantial investment. A deployment that uses another frequency band (e.g., 3.5

GHz) would still be useful, in terms of evaluating basic performance, testing feasibility of desired applications, and in terms of familiarizing investigators with the complex technology. The original basic plan for deployment (lab, then small airport, then large airport) is still a good one. Along with this plan should be a detailed test plan with clear milestones. In addition, a detailed channelization plan for partitioning the E-MLS band should be done.

A second recommendation is to explore the use of multiple antennas, for a multiple-input/multiple-output (MIMO) configuration. The use of even two antennas can bring substantial performance gains in the presence of severe channel fading. This is true even if multiple antennas can be used only at the 802.16 system base stations, and not on the mobile units. The use of so-called "mesh" or ad-hoc network deployments may also have some advantages in some situations, and so should be investigated. For both this and the MIMO case, this should begin with analysis and computer simulations, before actual deployment.

Another recommendation is that additional advanced processing techniques be explored. This was noted in the initial project objectives, and could involve frequency hopping and new adaptive data distribution algorithms. Both of these techniques would also improve system performance in the presence of interference. Exploring the use of new channel estimation algorithms could also enhance performance substantially, as our simulation results imply.

7. Acknowledgments

The principal investigator would like to thank the graduate students who assisted throughout this project. This includes former Ohio University Ph.D. students Indranil Sen and Beibei Wang, whose work on the channel models, and OFDMA simulations, respectively, were instrumental to the project. Also deserving of thanks is former Ohio University Ph.D. student Wenhui Xiong, who assisted with channel model and simulation development. Finally in this group is current OU Ph.D. student Kamalakar Ganti, who volunteered his time and effort on the enhanced coding and jamming studies.

The PI would also like to thank Michael Biggs of the FAA Spectrum Office for funding this work, and Rafael Apaza, of the Detroit FAA Field Office, for his continued support and persistent efforts to modernize airport surface communications.

8. References

[1] D. W. Matolak, "Development and Deployment of a Wireless Network Testbed and Evaluation of Wireless Systems for Airport Applications," proposal to the FAA Spectrum Office, January 2006.

[2] D. W. Matolak, B. Wang, "Development and Deployment of a Wireless Network Testbed, and Evaluation of Wireless Systems for Airport Applications," Interim Project report for FAA Grant # 06-G-005, December 2006.

[3] WiMax Forum, world wide web site, www.wimaxforum.org, July 2007.

[4] IEEE Military Communications Conference (*MILCOM 2006*), Washington, DC, 23-26 October 2006.

[5] IEEE 802 standards web site, http://grouper.ieee.org/groups/802/index.html , July 2007.

[6] ITT Industries, "Technology Assessment for the Future Aeronautical Communications System," NASA/CR-2005-213587, TR04055, Reston, VA, May 2005.
[7] J. G. Andrews, A. Ghosh, R. Muhamed, *Fundamentals of WiMAX: Understanding Broadband Wireless Networking*, Prentice-Hall, Upper Saddle River, NJ, 2007.
[8] D. W. Matolak, "Wireless Channel Characterization in the 5 GHz Microwave Landing System Extension Band for Airport Surface Areas," Final Project Report for NASA ACAST Project, Grant Number NNC04GB45G, May 2006.
[9] S. DeHart, "5 GHz E-MLS Band Partition Study," Sensis Corporation, 2006.
[10] R. Van Nee, R. Prasad, *OFDM for Wireless Multimedia Communications*, Artech House, Boston, MA, 2000.
[11] D. Parsons, *The Mobile Radio Propagation Channel*, Wiley, New York, NY, 1994.
[12] I. Sen, B. Wang, D. W. Matolak, "Performance of IEEE 802.16 OFDMA Standard Systems in Airport Surface Area Channels," to appear in *Proc. IEEE Fall Vehicular Tech. Conf.*, Baltimore, MD, 1-3 October 2007.
[13] J. G. Proakis, *Digital Communications*, 2nd ed., McGraw-Hill, New York, NY, 1989.
[14] A. Papoulis, S. U. Pillai, *Probability, Random Variables, and Stochastic Processes*, 4th ed., McGraw-Hill, New York, NY, 2002.
[15] G. Karagiannidis, et. al., "Equal Gain and Maximal Ratio Combining over Non-identical Weibull Fading Channels," *IEEE Trans. Wireless*, vol. 4, no. 3, pp. 841-846, May 2005.
[16] J. L. Burbank, W. T. Kasch, "IEEE 802.16 Broadband Wireless Technology and its Application to the Military Problem Space," *Proc. MILCOM '05*, Atlantic City, NJ, October 2005.
[17] J. Li, S. G. Haggman, "Performance Improvement of IEEE 802.16-2004 System in Jamming Environment via Link Adaptation," *Proc. MILCOM '06*, Washington, DC, October 2006.
[18] D. Matolak, I. Sen, W. Xiong, "Comparative Multicarrier System Performance in Jamming and Fading," *5th International Workshop on Multi-Carrier Spread Spectrum*, Oberpfaffenhofen, Germany, 14-16 Sept. 2005.
[19] Y. Zhou, Y. Fang, "Security of IEEE 802.16 in Mesh Mode," *Proc. MILCOM '06*, Washington, DC, October 2006.
[20] D. DeLuca, et. al., "Outdoor Path Loss Models for IEEE 802.16 in Suburban and Campus Like Environments," *Proc. IEEE ICC*, Glasgow, Scotland, UK, June 2007.
[21] C. Heegard, S. B. Wicker, *Turbo Coding*, Kluwer Academic Publishers, Boston, MA, 1998.
[22] A. J. Goldsmith, S. G. Chua, "Variable-Rate Variable-Power M-QAM for Fading Channels," *IEEE Trans. Comm.*, vol. 45, no. 10, pp. 1218-1230, October 1997.